In-plane and out-of-plane mechanical characterization of thin polysilicon

F. Cacchione[*], B. De Masi[**], A. Corigliano[*], M. Ferrera[**], A. Vinay[**]

[*]Department of Structural Engineering, Politecnico di Milano, Piazza L. da Vinci 32, 20133 Milano, Italy, cacchione@stru.polimi.it, alberto.corigliano@polimi.it
[**]MEMS Business Unit, STMicroelectronics,Via Tolomeo 1, 20010 Cornaredo (Milano), Italy, biagio.demasi@st.com

ABSTRACT

Elastic stiffness and strength of thin polysilicon films were obtained through on-chip test structures with in plane and out of plane loading conditions. Comparative studies were performed to investigate the variation of the ultimate strength of the polysilicon film (caused by the cristalline structure of the material) with different loading conditions.

Keywords: polysilicon, MEMS, reliability, Young's modulus, tensile strength

1 INTRODUCTION

The recent development of MEMS technology (see e.g. [1]) and the diffusion of these devices in various applications has forced many researchers to tackle the important issue of MEMS reliability. References [2]-[7] are only examples of various possible approaches conceived to determine mechanical properties of polysilicon like e.g. the Young's modulus, the tensile strength and fracture toughness.

The Authors have recently developed and discussed (see e.g. [8]-[10]) an on-chip approach for the mechanical characterization of thin polysilicon films. Various devices have been designed and produced which load up to rupture in tensile or bending conditions small polysilicon specimens by means of electrostatic actuation.

The aim of the present paper is to present and discuss recent results concerning the mechanical behaviour of thin polysilicon films loaded in bending up to rupture by means of two different devices. The first device loads a couple of doubly clamped beams in bending in the plane parallel to the substrate, while the specimens in the second device are loaded in bending in the plane orthogonal to the substrate.

Experimental results obtained from the two actuators are important for a discussion on possible effects of the polysilicon structure on its mechanical behaviour.

An outline of the paper is as follows. In Section 2 the layout and the main properties of the in-plane rotational electrostatic actuator are briefly described. The out-of plane actuator is described in Section 3. Section 4 is devoted to the description of the experimental setup and of the data reduction procedure. The first obtained experimental results are discussed in Section 5. Section 6 contains some closing remarks.

2 ROTATIONAL TEST STRUCTURE

The device shown in Fig. 1 is made of a central ring connected to the substrate by means of two tapered 0.9 μm thick specimens which also act as suspension springs of the whole system. Rigidly connected to the central ring are 12 arms with a total of 384 comb fingers capacitors which move, due to the electrostatic attraction, towards the stators rigidly connected to the substrate. When a voltage is applied to the device, the comb fingers develop a force distributed along the 12 arms, equivalent to a torque applied to the central ring. This in turn loads the two specimen in bending in the plane parallel to the substrate. The force developed by the system of comb fingers is sufficient to load the specimens up to rupture.

The specimens are a pair of doubly clamped slender beams, with a length of 34 μm and a trapezoidal cross-section (see a detail in Fig. 2). Their width decreases linearly from 5.3 μm to 1.8 μm. This shape was *ad hoc* designed in order to localize the fracture of the specimen in a specified area through stress concentration.

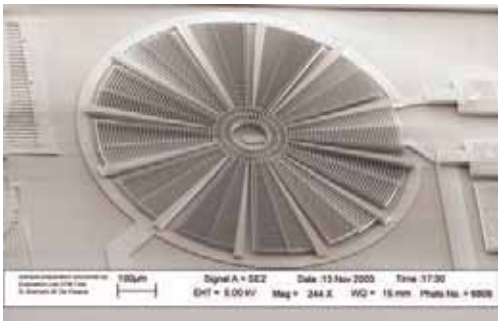

Figure 1: In-plane rotational actuator, general view

Figure 2: In plane rotational actuator, specimens

3 OUT OF PLANE TEST STRUCTURE

The holed plate of 15 μm thick polysilicon shown in Fig. 3 is suspended on the substrate by means of four elastic springs placed at the four corners. The holed plate is also connected to the thin polysilicon film specimens placed at the centre, as shown in Fig. 4. The two symmetric specimens, 0.9 μm thick, are in turn connected on one side to the holed plate, while on the other are rigidly connected to the substrate. The two specimens are therefore equivalent to a couple of doubly clamped beams. The holes in the plate are due to the etching process for the elimination of the sacrificial layer, thus allowing for movement of the holed plate with respect to the substrate.

The movement in the direction orthogonal to the substrate is obtained by electrostatic attraction of the holed plate towards the substrate. The whole plate and the substrate thus act as a parallel plate electrostatic actuator. When the plate moves towards the substrate, the couple of specimens bend.

It is important to remark that only the squared part of the holed plate act as an actuator (see Fig. 3), while the holed rectangular parts added to each side of the plate act as sensors; these in turn allow for the experimental determination of capacitance variation and vertical movement, as discussed in Section 4.

The length of each specimen is 7. μm; as in the rotational actuator, in order to force the rupture in a priori chosen section, their cross section changes with a linearly varying width which decreases from 3. μm to 1. μm (see Fig. 4).

4 EXPERIMENTAL SETUP AND DATA REDUCTION PROCEDURE

Tests were carried out at room temperature and at atmospheric humidity, with a probe station mounted on an optical microscope. The experimental setup is schematically shown in Fig. 5. The input voltage given to the structure and the variation of the capacitance induced by the rotation of the rotor were measured connecting an Agilent Precision 4284A LCR Meter between two pads. The LCR resolution, in the range of measures of interest in this work, is $\pm 1 fF$. The LCR-meter and the substrate were grounded together. The wafer was accurately positioned on an electromagnetically shielded measurement table and the electric connection on the MEMS pads was micrometrically tuned.

A slowly increasing voltage was applied in order to induce quasi static loading conditions in the specimen. The data reduction procedure, similar for the two actuators, was based on analytical and Finite Element (FE) results, as briefly described here below.

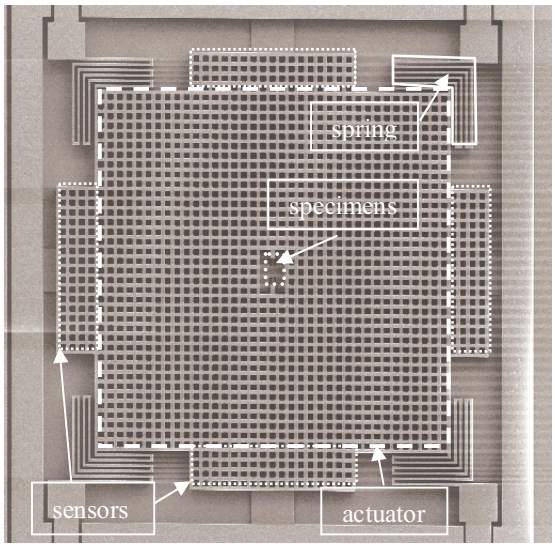

Figure 3: Out of plane parallel actuator, general view

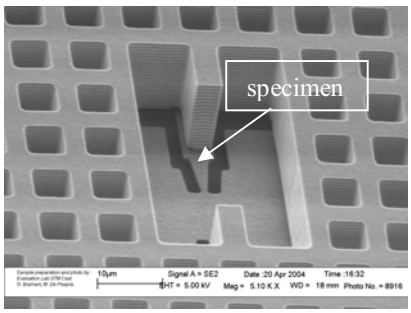

Figure 4: Out of plane parallel actuator, specimens

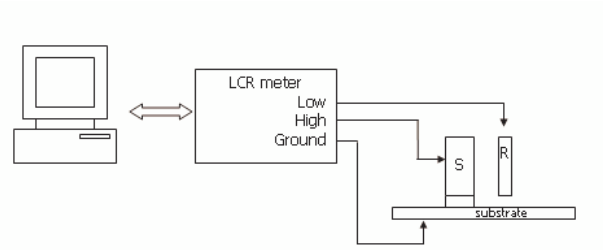

Figure 5: Scheme of the experimental setup

Rotational actuator

Analytical formula for comb finger actuators were used in order to obtain from the given voltage the torque applied to the central ring and from the measured capacitance variation the rotation of the central ring. An example of global torque versus global rotation plot is shown in Fig. 6. Starting from the torque-rotation plots, the Young's modulus and the rupture strength were finally obtained by making use of 3D linear elastic finite element simulations. A detailed description of the data reduction procedure applied for the rotational device can be found in the extended version of paper [9].

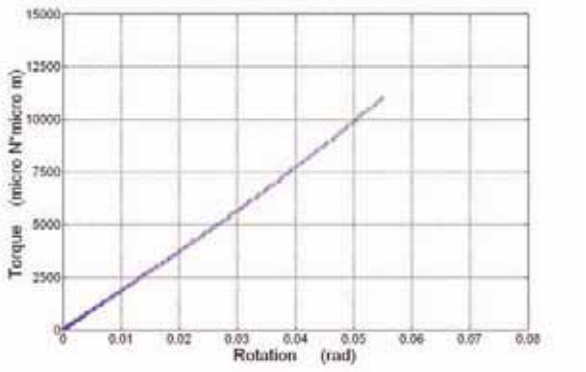

Figure 6: Rotational actuator, example of torque versus rotation plot.

Holed plate actuator

The experimentally determined capacitance vs. voltage plots were transformed in force vs. displacement plots by making use of relationships between capacitance and displacement and between voltage and electrostatic force, respectively. The first were derived from a series of electrostatic Boundary Elements (BE) simulations on one of the lateral sensors which allowed for the determination of a capacitance variation versus vertical gap plot.

FE electrostatic simulations were used in order to obtain the vertical force of attraction on the square holed plate acting as a rotor. From the results of FE electrostatic simulations it was deduced that the attractive vertical force can be computed by making use, with negligible error, of the analytical relation for a parallel plate actuator with the same surface and with the correction due to edge fringing effects.

By means of the above briefly described procedure, the experimental capacitance vs. voltage plot was transformed for each test in a force vs. displacement one, as in the example shown in Fig. 7.

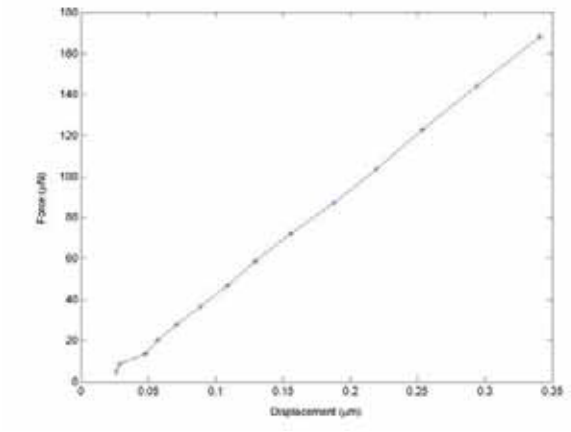

Figure 7: Parallel plate actuator, force-displacement plot obtained after the data reduction procedure

Starting from the force-displacement plot, the force acting on the specimens was obtained by subtracting the part equilibrated by the elastic suspension springs in the four corners of the holed plate (see Fig. 3). An elastic 3D FE solution of the specimen under bending in the vertical plane was then used to relate the global stiffness of the specimen to the Young's modulus and the force at rupture to the maximum tensile stress in the specimen. Experimental values of Young's modulus and rupture stress were therefore finally obtained. More details on the data reduction procedure can be found in [10].

5 RESULTS

As briefly discussed in the previous Section, Young's modulus and tensile rupture strength were obtained with the two on-chip devices described in Sections 2 and 3. A summary of the main results is given here below.

Rotational actuator

The measured Young's modulus obtained after 92 tests was 175 $\pm$ 4 *GPa*. The low dispersion around the mean value confirms the quality and good reliability of the whole procedure (Fig. 8).

The rupture strength was obtained after 75 tests; the measured rupture strength directly given by the data reduction procedure described in Section 4, was 2898 $\pm$ 325. *MPa.* Weibull parameters obtained taking into account stress gradient effects and size effects, as discussed in the extended version of [15], were σ_0 = 2234 *MPa*, m = 10.3.

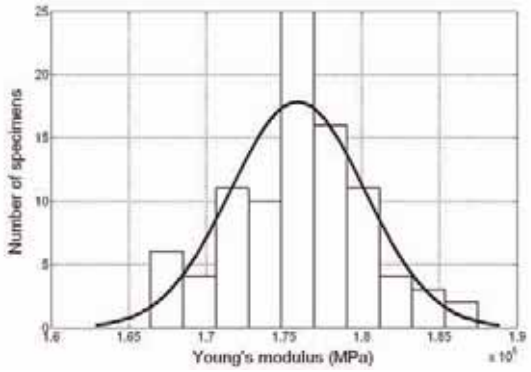

Figure 8: Rotational actuator, experimental distribution of Young's modulus

Holed plate actuator

The Young's modulus obtained after 19 tests was 169 $\pm$ 11 *GPa*. Also in this case a low dispersion around the mean value confirms the quality and good reliability of the whole procedure (Fig. 9).

The rupture strength obtained after 25 tests was 7447 $\pm$ 483 *MPa*. Weibull parameters obtained taking into account

stress gradient effects and size effects, were σ_0 = 5276 *MPa*, m = 18.2.

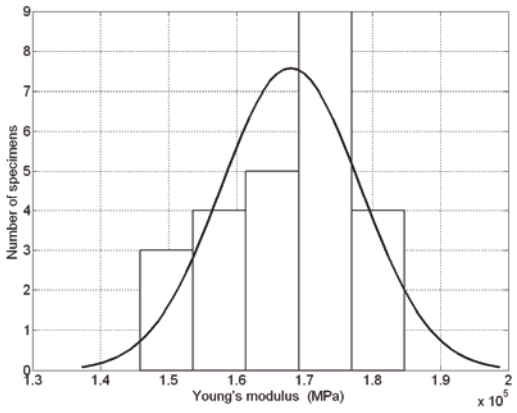

Figure 9: Parallel plate actuator, experimental distribution of Young's modulus

The values of Young's modulus obtained by means of the two on-chip test devices can be considered coincident. The out-of plane loading shows a larger dispersion. The fact that the two values coincide seem to confirm the homogeneity of the thin polysilicon along the thickness.

As also discussed in [10], the difference in the rupture strength values cannot be considered negligible and should be carefully examined and discussed. It could be only partially attributed to a greater influence of defects distributed on the vertical sides than those distributed on the surfaces of the specimen parallel to the substrate. The Authors consider these results only preliminary and wish to carefully examine the whole data reduction procedure for the out of plane actuator.

6 CONCLUSION

Young's modulus and rupture strength of 0.9 μm polysilicon specimens were determined by means of two different on-chip electrostatic actuators. The first one loads a couple of doubly clamped beams in bending in the plane parallel to the substrate; the second one loads similar specimens in the plane orthogonal to the substrate.

The different loading conditions does not seem to affect the value of Young's modulus, while apparently give a remarkable difference in the values of rupture strength. It is the Authors' opinion that the rupture values obtained by means of the parallel plate, out of plane device must be considered only partial, the whole procedure of data reduction and the failure mechanisms deserve careful examination.

Acknowledgments

The contribution of EU NoE Design for Micro & Nano Manufacture (PATENT-DfMM), contract n°: 507255 is gratefully acknowledged.

REFERENCES

[1] S.E. Lyshevski, "MEMS and NEMS, Systems Devices and Structures", CRC Press, Boca Raton, 2002.

[2] P.M. Oostemberg and S.D. Senturia, "M-Test: a test chip for MEMS material property measurement using electrostatically actuated test structures", Journal of Microelectromechanical Systems, 6, 107-118, 1997.

[3] H. Kahn, N. Tayebi, R. Ballarini, R.L. Mullen and A.H. Heuer, "Fracture toughness of polysilicon MEMS devices", Sensors and Actuators, 82, 274-280, 2000.

[4] T. Ando, M. Shikida, K. Sato, "Tensile-mode fatigue testing of silicon films as structural material for MEMS", Sensor and Actuators A, 93, 70-75, 2001.

[5] I. Chasiotis, W.G. Knauss, "A New Microtensile Tester for the Study of MEMS Materials with the aid of Atomic Force Microscopy", Experimental Mechanics, 42(1), 51-57, 2002.

[6] J. Bagdahn, W.N. Sharpe Jr, "Fracture strength of polysilicon at stress concentrations", Journal of Microelectromechanical Systems, 12, 302-312, 2003.

[7] D. Gao, C. Carraro, V. Radmilovic, R.T. Howe, "Fracture of polycrystalline 3C-SiC films in microelectromechanical systems", J. of Microelectromechanical Systems, 13, 6, 972-976 2004.

[8] A. Corigliano, B. De Masi, A. Frangi, C. Comi, A. Villa, M. Marchi, "Mechanical characterization of polysilicon through on chip tensile tests", J. of Microelectromechanical Systems, 13, 2, 200-219 2004.

[9] F. Cacchione, B. De Masi, A. Corigliano, M. Ferrera, "Rupture tests on polysilicon films through on-chip electrostatic actuation", Proceedings: Eurosime04, Brussels, 9-12 May 2004. Extended version submitted to Sensor Letters, 2005.

[10] F. Cacchione, A. Corigliano, B. De Masi, M. Ferrera, "Out of plane flexural behaviour of thin polysilicon films: mechanical characterization and application of the Weibull approach", Proceedings: Eurosime05, Berlin, 18-20 April 2005.